A biosystems approach to identify the molecular signaling mechanisms of TMEM30A during tumor migration

Jiao Wang[1]ʘ, Qian Wang[1]ʘ, Dongfang Lu[2], Fangfang Zhou[1], Dong Wang[1], Ruili Feng[1], Kai Wang[3], Robert Molday[4], Jiang Xie[2]*, Tieqiao Wen[1]*

1 Laboratory of Molecular Neural Biology, School of Life Sciences, Shanghai University, Shanghai, China, **2** School of Computer Engineering and Science, Shanghai University, Shanghai, China, **3** Shanghai Key Laboratory of Molecular Andrology, Institute of Biochemistry and Cell Biology, Shanghai Institute of Biological Science, Chinese Academy of Sciences, Shanghai, China, **4** Department of Biochemistry and Molecular Biology, University of British Columbia, Vancouver, Canada

ʘ These authors contributed equally to this work.
* jiangx@shu.edu.cn (JX); wtq@shu.edu.cn (TQW)

Abstract

Understanding the molecular mechanisms underlying cell migration, which plays an important role in tumor growth and progression, is critical for the development of novel tumor therapeutics. Overexpression of transmembrane protein 30A (TMEM30A) has been shown to initiate tumor cell migration, however, the molecular mechanisms through which this takes place have not yet been reported. Thus, we propose the integration of computational and experimental approaches by first predicting potential signaling networks regulated by TMEM30A using a) computational biology methods, b) our previous mass spectrometry results of the TMEM30A complex in mouse tissue, and c) a number of migration-related genes manually collected from the literature, and subsequently performing molecular biology experiments including the *in vitro* scratch assay and real-time quantitative polymerase chain reaction (qPCR) to validate the reliability of the predicted network. The results verify that the genes identified in the computational signaling network are indeed regulated by TMEM30A during cell migration, indicating the effectiveness of our proposed method and shedding light on the regulatory mechanisms underlying tumor migration, which facilitates the understanding of the molecular basis of tumor invasion.

Introduction

Migration and invasion are key behaviors that distinguish benign from malignant tumors, enabling cell metastasis across tissue boundaries from the primary tumor location to a distant secondary site [1], thereby increasing disease severity and therapeutic challenges. Great effort, therefore, has been exerted to elucidate the mechanisms underlying cell migration and invasion [2–4]. Numerous studies have confirmed that invasive carcinoma cells acquire a migratory phenotype associated with various molecular and cellular mechanisms involved in cancer

cell invasion [5, 6]. Tumor cell invasion is initiated by the loss of the cell-cell adhesion capacity from the primary tumor mass, and subsequent, changes in cell-matrix interactions enable the cells to invade surrounding tissue [4, 7]. Pathology observations *in vivo* indicate that tumor cells migrate in two main ways: individually and collectively [4, 8], knowledge of which has attracted efforts focusing on cell adhesion, epithelial to mesenchymal transition, angiogenesis, lymphangiogenesis and organ-specific metastasis [7]. Moreover, related molecules including cell adhesion factors [9, 10], growth factors [11], microRNA [3, 12], and lncRNA [13, 14] has been reported to be active during the metastatic cascade. Mounting evidence also indicates that inaddition to internal molecules, external influences modulate tumor migration and invasion [1, 2, 7, 15], such as chemical signals [16] and excessive amounts of exosomes released by tumor cells [17]. Nevertheless, the elaborate and complex regulatory mechanisms involved in the control of tumor cell migration remain unclear [1, 2, 7, 18].

TMEM30A is a terminally-glycosylated membrane protein that is ubiquitously expressed in mouse tissue [19]. The TMEM30A phospholipid flippase complex is known to play a role in cell migration [20] via the formation of membrane ruffles as a result of phospholipid translocation. However, it remains to be determined which molecules within the migratory machinery coordinate functions with this complex. In the present study, we aim to explore the molecular signaling mechanisms of TMEM30A using a biosystems approach to identify the signaling networks involved in tumor migration (S1 Fig). Our proposed method integrates computational and experimental approaches by first predicting potential signaling networks regulated by TMEM30A using computational biology methods, and subsequently performing molecular biology experiments including the *in vitro* scratch assay and qPCR. We assume that, in order to affect tumor migration, TMEM30A must regulate the expression of migration-related genes through certain pathways. The migration signaling network was constructed based on the STRING database together with our previous mass spectrometry results of the TMEM30A complex in mouse tissue and a number of migration-related genes manually collected from the literature. Subsequently, using both published data and our experimental results, the genes in the computationally-identified signaling network were validated and indeed shown to be regulated by TMEM30A during tumor migration, laying the foundation for the development of a potential cancer therapy.

Materials and methods

Computational prediction of the molecular mechanisms involved in migration

To identify signaling pathways regulated by TMEM30A during tumor migration, a number of migration-related genes were first manually collected from the literature. Subsequently, we obtained the protein-protein interaction network (PPIN) for *Mus musculus* from the STRING 10.0 database containing all known and predicted protein-protein interactions. In this version, there are 22668 distinct protein-encoding genes and 5109107 interactions, with weights between 1 and 999. The greater the weight, the higher the confidence, and the stronger the interaction. Subsequently, our previous mass spectrometry results of the TMEM30A complex in mouse tissue and the known migration-related genes from the literature were superimposed onto the PPIN from the STRING database. The sub-network of these selected proteins were extracted from the whole PPIN in STRING, which includes 377 proteins and 14161 interactions. DAVID was used to conduct the function and pathway enrichment analysis and the signaling network was visualized with Cytoscape [21]. http://dx.doi.org/10.17504/protocols.io.iapcadn [PROTOCOL DOI]

Cell culture

Human hepatocellular carcinoma, SMMC-7721, and cervical adenocarcinoma, HeLa, cell lines were obtained from the Cell Bank of the Chinese Academy of Sciences (Shanghai, China). The cells were cultured in RPMI 1640 medium (Gibco, USA) supplemented with 10% fetal bovine serum (Hyclone, USA) and 1% penicillin/streptomycin (Gibco, USA). Maintenance was carried out under 5% CO_2, in a 95% humidified atmosphere at 37˚C. When the cells reached approximately 90% confluency, they were detached with 0.1% trypsin—ethylenediamine tetraacetic acid (Gibco, USA), seeded onto appropriate dishes, and incubated overnight. http://dx.doi.org/10.17504/protocols.io.iaqcadw [PROTOCOL DOI]

Gene transfection

Transfection was carried out using *Lipofectamine*™ 2000 transfection reagent (Invitrogen, 12566014), according to the protocol provided. Briefly, cells were seeded in 24-well plates at a density of 1×10^5 cells/500 μl and cultured overnight. 0.5 μg pcDNA3-ATP11A and 0.5 μg pcDNA3-TMEM30A plasmids in *Lipofectamine*™ 2000-RPMI 1640 medium (W/V, 1:1) (50 μl) were added dropwise to the cells, which were subsequently incubated under 5% CO_2 in a 95% humidified atmosphere at 37˚C for 6 h, following which the medium was replaced with fresh. http://dx.doi.org/10.17504/protocols.io.iarcad6 [PROTOCOL DOI]

Measurement of cell migration

Cells were seeded at a density of 1×10^5 cells/well in a 24-well plate and cultured under 5% CO_2 at 37˚C for 24 h. Following 6 h transfection, changes in the rate of cell migration were measured using a wound healing assay. Briefly, cells in each well were separated by a scratch-wound, a standardized scratch made with a P-20 pipette tip, and cells were observed every 12 h for 48 h using a Nikon Ti-S fluorescence microscope. The data were analyzed using the Image-Pro Plus software. http://dx.doi.org/10.17504/protocols.io.iascaee [PROTOCOL DOI]

Total RNA extraction, cDNA synthesis, and qPCR

Cells were cultured in 24-well plates. 48 h post-transfection, the total cellular RNA was extracted using a Total RNA Extraction Kit (Promega, USA), according to the manufacturer's protocol. The concentration of RNA was determined by measuring the absorbance at 260 nm, and 2 μg RNA was used for cDNA synthesis using an RT Master Mix (TaKaRa, Japan). qPCR amplification was performed using a mixture of Top Green qPCR Super Mix (Transgen, China), cDNA samples, and designated primers (Table 1). Relative gene expression was calculated by comparison of the CT value of the gene of interest with that of GAPDH, the internal control. http://dx.doi.org/10.17504/protocols.io.iaucaew [PROTOCOL DOI]

Statistical analysis

All data were analyzed using the GraphPad Prism software and are presented as the mean ± SEM. Average gaps in the cell migration assay were measured using the Image-Pro Plus software, and the rate of cell migration was analyzed by a two-way ANOVA. The mRNA level was analyzed by a one-way ANOVA. $P < 0.05$ is considered statistically significant.

Table 1. List of primers used in qPCR.

Gene name	Primer sequence (5' to 3')
GAPDH	Upstream: TCACCACCATGGAGAAGGC
	Downstream: GCTAAGCAGTTGGTGGTGCA
SRC	Upstream: GAACCCGAGAGGGACCTTC
	Downstream: GAGGCAGTAGGCACCTTTTGT
CDC42	Upstream: CCATCGGAATATGTACCGACTG
	Downstream: CTCAGCGGTCGTAATCTGTCA
WASL	Upstream: CCCCAAATGGTCCTAATCTACCC
	Downstream: TGGAAATTGCTTGGTGTTCCTAT
RHO	Upstream: GGAAAGCAGGTAGAGTTGGCT
	Downstream: GGCTGTCGATGGAAAAACACAT
SUB1	Upstream: GAAGGTGAAATGAAACCAGGAAG
	Downstream: ACAGCTTTCTTACTGCGTCATC
SLC2A1	Upstream: GGCCAAGAGTGTGCTAAAGAA
	Downstream: CGATACCGGAGCCAATGGT
CTNNB1	Upstream: TGATGGAGTTGGACATGGCCATGGA
	Downstream: TGGCACCAGAATGGATTCCAGA
ACTB	Upstream: GTGACGTTGACATCCGTAAAGA
	Downstream: ATGAAGATCAAGATCATTGCTCCT
HSP90B1	Upstream: CAGAGAGAGGAAGAAGCTATTCAG
	Downstream: TTAAAAACTCGCTTGTCCCAGAT
CLTC	Upstream: AATGAAGGCCCATACCATGACT
	Downstream: TTATCCGTAACAAGAGCAACCG

Results

Construction of the molecular signaling networks involved in the TMEM30A complex

In order to identify the molecular signaling networks involved in TMEM30A, our previous mass spectrometry results of the TMEM30A complex in mouse tissue and the known migration-related genes from the literature were superimposed onto the PPIN from the STRING database, since PPIN is widely used for the identification of signal transduction pathways. The largest connected component in the PPIN, consisting of 347 migration-related genes and 14161 interactions, was constructed for further analysis. To elucidate the most-related genes, the first neighbors of TMEM30A were selected, which formed a small network of 49 genes with 493 interactions (Fig 1). Moreover, migration-related genes were manually collected from the literature, of which 14 are found in the above PPIN (Table 2).

Investigation of the functions of these genes is shown in Fig 1. We found that phospholipid and proton transport are significantly enriched (18 out of 49 genes) in the network, demonstrating that these genes are likely related to cell migration. SLC2A1, for instance, is critical for the growth and proliferation of tumor cells, with high SLC2A1 expression being associated with increased migration and poor patient survival [22]. Moreover, knockdown of SEC23A, a GTPase-activating protein critical for protein trafficking, has been shown to increase the proliferation, migration, and invasion of colorectal cancer cells [23]. Table 3 lists the top 20 most enriched functions of the genes in the identified signaling network, in which the biological process category from Gene Ontology was considered. Further, the enriched pathways from the KEGG database were screened for the genes in our predicted signaling network (Table 4).

Fig 1. The migration-related signaling network regulated by TMEM30A. The largest connected components in the PPIN consisting of 347 genes expressed during migration and 14161 interactions. The first neighbors of TMEM30A were selected and a small network including 49 genes and 493 interactions was formed. The inner circles denote migration-related genes manually collected from the literature. The outer circles denote the genes predicted to interact with TMEM30A. The purple nodes were randomly-selected for experimental validation by qPCR.

Among the 20 enriched pathways were those involved in the regulation of the actin cytoskeleton, adherens junctions, and focal adhesion, which are already known to be related to migration. From both the functional and pathway enrichment analyses, it can be seen that our identified signaling network including TMEM30A is indeed related to tumor migration.

Identification of the overexpression of TMEM30A and ATP11A

To further verify that our predicted signaling network is indeed regulated by TMEM30A, we investigated its effects on several randomly selected genes by manipulating TMEM30A expression. TMEM30A structurally resembles the β-subunit of the P4-ATPase, which is abundant in our mass spectra (Fig 1), and is also responsible for the preservation of lipid gradients in mammalian tissues [24], thus ATP11A, a member of the P4-ATPase family, was selected since it has been reported to be a novel predictive marker for colorectal cancer prognosis [25]. TMEM30A and ATP11A were therefore overexpressed in two different human tumor cell

Table 2. The 14 known migration-related genes.

Gene symbol	Description	References (PIMID)
PIK3CA	Phosphatidylinositol 3-kinase, catalytic, alpha polypeptide	22064833; 27465249; 26829882; 27489350; 27511117; 27001433; 26747178; 25958091; 27460294; 28123856
RASA1	RAS p21 protein activator 1	25520857; 27101583; 26747707; 25778421; 21768288; 14639529
CRK	V-crk avian sarcoma virus CT10 oncogene homolog	27974675; 27656905; 27703373; 27418680; 27242434; 27210447; 27133071; 27052191
SRC	Rous sarcoma oncogene	27226554; 26773066; 24127286; 25711940; 24197068; 25870166; 27698945; 26645362
WASL	Wiskott-Aldrich syndrome-like	25621495; 24480980; 26500649; 19760510; 26656091; 22084245
ARHGDIA	Rho GDP dissociation inhibitor (GDI) alpha	27841340; 27726098; 26761212; 26062653; 25961457; 24859471; 24240172; 23867502; 22960606; 22928040
ACTR2	ARP2 actin-related protein 2	26370503; 24918434; 23644663; 16051170; 16004967; 15894313; 15727206
WIPF1	WAS/WASL interacting protein family, member 1	27863429; 26563365; 25169059; 18755005; 22823953; 17949983; 17312144; 16546573
CDC42	Cell division cycle 42	26450120; 25160664; 26634649; 23861058; 23562274; 23727359; 26633832; 26926567
RDX	Radixin	26438043; 24464681; 22199287; 22179828; 23339187; 22445717; 20739942; 15212902
ACTR3	ARP3 actin-related protein 3	26370503; 25682201; 24385601; 22370639; 16051170; 28115943; 16004967
RHO	Rhodopsin	28182100; 28143875; 28143705; 28135625; 28130497; 28123576; 28119242; 28115390
ROCK1	Rho-associated coiled-coil containing protein kinase 1	28123850; 28123576; 28115943; 28112365; 28054559; 27881000; 27852062; 27841867; 27666391
MAPK1	Mitogen-activated protein kinase 1	26346167; 26955781; 26514298; 26968871; 26945151; 26117268; 23051912; 26443721; 25770213; 25655003

lines, hepatocellular carcinoma SMMC-7721 and cervical adenocarcinoma HeLa. Green fluorescence images revealed that overexpression plasmids were efficiently transfected into 7721 (Fig 2A) and HeLa cells (Fig 2B), respectively. In the qPCR results, the mRNA expression levels of ATP11A and TMEM30A were significantly increased in both 7721 (Fig 2C) and HeLa cells (Fig 2D). These results indicated that TMEM30A and ATP11A were successfully overexpressed in these two cancer cell lines.

Tumor migration mediated by TMEM30A

A wound-healing assay was conducted to assess the effect of TMEM30A and ATP11A on 7721 or HeLa cell migration. Representative images of the scratched areas in each condition at different time points were photographed. The results showed that the scratched areas in both 7721 (Fig 3A) and HeLa (Fig 3B) cells decreased from 12 to 48 h. Moreover, statistical analysis revealed that the migration rate of 7721 cells was significantly increased from 24 h in the ATP11A+TMEM30A group (Fig 3C). Similarly, the migration rate of HeLa cells also dramatically increased from 12 h in the ATP11A+TMEM30A group (Fig 3D). Taken together, overexpression of TMEM30A and ATP11A led to a significant increase in the migration rate of both 7721 and HeLa cells, indicating that TMEM30A is involved in cell migration.

Experimental validation of the signaling network

As can be seen in Fig 4A and 4B, four genes, SRC, CDC42, WASL, and RHO were selected from 14 genes (Table 2) that had already been confirmed to be related to migration. The mRNA levels of CDC42, WASL, and RHO were significantly increased in 7721 cells. However,

Table 3. The top 20 most enriched functions of the genes in the predicted signaling network regulated by TMEM30A, where the biological process from Gene Ontology was considered.

Function	P-value	Genes in the predicted signaling network
Transport	1.06×10^{-6}	SEC23A, ATP1A3, ATP11A, ATP1A1, ATP11C, ABCA4, CNGA1, ATP6V1A, SRSF7, COPB1, ARF4, SLC2A1, ATP8A2, SEC22B, ATP5A1, DYNC1I2, TMEM30A, ATP8A1
Phospholipid transport	1.61×10^{-6}	ATP8A2, ATP11A, ATP11C, TMEM30A, ATP8A1
Ephrin receptor signaling pathway	4.21×10^{-6}	CDC42, WASL, CRK, SRC, RASA1
Spindle localization	6.30×10^{-5}	ACTR3, ACTR2, WASL
ATP hydrolysis-coupled proton transport	7.97×10^{-5}	ATP6V1A, ATP1A3, ATP1A1, ATP5A1
Lipid transport	1.80×10^{-4}	ATP8A2, ATP11A, ATP11C, TMEM30A, ATP8A1
Adherens junction organization	2.25×10^{-4}	CDC42, SRC, CTNNB1
Phospholipid translocation	3.43×10^{-4}	ATP11C, ABCA4, TMEM30A
Actin filament organization	1.23×10^{-3}	ACTR3, ACTR2, CDC42, WASL
Cellular response to platelet-derived growth factor stimulus	1.55×10^{-3}	RDX, SRC, RASA1
Vesicle-mediated transport	2.07×10^{-3}	SEC23A, COPB1, ARF4, SEC22B, CLTC
Establishment or maintenance of cell polarity	2.13×10^{-3}	ACTR3, ACTR2, CDC42
Meiotic cytokinesis	5.08×10^{-3}	ACTR3, ACTR2
Actin cytoskeleton organization	5.62×10^{-3}	ACTR2, ROCK1, WASL, WIPF1
Rho protein signal transduction	6.10×10^{-3}	CDC42, ROCK1, ARHGDIA
Asymmetric cell division	7.61×10^{-3}	ACTR3, ACTR2
Positive regulation of phospholipid translocation	7.61×10^{-3}	ATP8A2, ATP8A1
Meiotic chromosome movement towards spindle pole	7.61×10^{-3}	ACTR3, ACTR2
Fc-gamma receptor signaling pathway involved in phagocytosis	1.01×10^{-2}	CDC42, WASL
Response to drugs	1.07×10^{-2}	ATP1A3, ATP1A1, SRC, RASA1, CTNNB1

https://doi.org/10.1371/journal.pone.0179900.t003

in HeLa cells, the mRNA expression of *SRC* was significantly increased, and that of *WASL* was dramatically decreased. As shown in Fig 4C and 4D, another 6 genes, *SUB1*, *SLC2A1*, *CTNNB1*, *ACTB*, *HSP90B1*, and *CLTC* were selected from the remaining unknown migration-related genes in order to confirm their relationship with cancer cell migration. In the present study, the results show that the mRNA levels of *SUB1*, *SLC2A1*, *CTNNB1*, *ACTB*, and *CLTC* were increased in 7721 cells but decreased in HeLa cells, with the exception of *ACTB*, which was also significantly increased. Moreover, the products of the qPCR were subjected to agarose gel electrophoresis to reflect the abundance of each mRNA transcript in 7721 (Fig 4E) or HeLa cells (Fig 4F), which were consistent with above results.

Discussion

In recent years, many research groups have become interested in investigating pathways from protein-protein interaction and high-throughput data, with various computing methods having been developed to indicate molecular pathways [26–28]. In this work, we obtained the protein-protein interaction data for *Mus musculus* from the STRING database 10.0, which is an open source database for all known and predicted protein-protein interactions. Subsequently, the proteins from our previous TMEM30A complex mass spectrometry experiment in mouse tissue and a number of manually collected migration-related proteins were superimposed onto

Table 4. Pathway enrichment analysis of genes in the predicted signaling network regulated by TMEM30A, where the pathway information was obtained from the KEGG database.

Pathway	P-value	Genes in the predicted signaling network
Bacterial invasion of epithelial cells	2.83×10^{-8}	ACTB, CDC42, PIK3CA, WASL, CLTC, CRK, SRC, CTNNB1
Thyroid hormone signaling pathway	3.73×10^{-7}	ACTB, MAPK1, SLC2A1, ATP1A3, PIK3CA, ATP1A1, SRC, CTNNB1
Regulation of actin cytoskeleton	2.34×10^{-6}	ACTB, MAPK1, CDC42, ROCK1, PIK3CA, RDX, WASL, CRK, SRC
Adherens junctions	1.19×10^{-5}	ACTB, MAPK1, CDC42, WASL, SRC, CTNNB1
Salmonella infection	1.76×10^{-5}	ACTB, MAPK1, CDC42, ROCK1, WASL, DYNC1I2
Proteoglycans in cancer	1.87×10^{-5}	ACTB, MAPK1, CDC42, ROCK1, PIK3CA, RDX, SRC, CTNNB1
Focal adhesion	2.13×10^{-5}	ACTB, MAPK1, CDC42, ROCK1, PIK3CA, CRK, SRC, CTNNB1
cGMP-PKG signaling pathway	7.29×10^{-5}	MAPK1, ROCK1, ATP1A3, PPP3CB, PIK3CA, ATP1A1, CNGA1
VEGF signaling pathway	1.14×10^{-4}	MAPK1, CDC42, PPP3CB, PIK3CA, SRC
Chemokine signaling pathway	1.55×10^{-4}	MAPK1, CDC42, ROCK1, PIK3CA, WASL, CRK, SRC
Renal cell carcinoma	1.75×10^{-4}	MAPK1, CDC42, SLC2A1, PIK3CA, CRK
Rap1 signaling pathway	2.50×10^{-4}	ACTB, MAPK1, CDC42, PIK3CA, CRK, SRC, CTNNB1
Fc gamma R-mediated phagocytosis	4.20×10^{-4}	MAPK1, CDC42, PIK3CA, WASL, CRK
Oxytocin signaling pathway	5.03×10^{-4}	ACTB, MAPK1, ROCK1, PPP3CB, PIK3CA, SRC
Aldosterone-regulated sodium reabsorption	6.31×10^{-4}	MAPK1, ATP1A3, PIK3CA, ATP1A1
Pathways in cancer	1.20×10^{-3}	MAPK1, CDC42, HSP90B1, ROCK1, SLC2A1, PIK3CA, CRK, CTNNB1
cAMP signaling pathway	1.36×10^{-3}	MAPK1, ROCK1, ATP1A3, PIK3CA, ATP1A1, CNGA1
Leukocyte transendothelial migration	1.65×10^{-3}	ACTB, CDC42, ROCK1, PIK3CA, CTNNB1
Neurotrophin signaling pathway	1.70×10^{-3}	MAPK1, CDC42, PIK3CA, CRK, ARHGDIA
Axon guidance	2.09×10^{-3}	MAPK1, CDC42, ROCK1, PPP3CB, RASA1

https://doi.org/10.1371/journal.pone.0179900.t004

the PPIN to elucidate the signaling mechanisms of TMEM30A during tumor migration. Our results indicate that TMEM30A and ATP11A promote the migration of tumor cells (Fig 3), which is consistent with reports that depletion of either TMEM30A or ATP8A1 causes a severe defect in cell migration [20]. Taken together, it can be speculated that TMEM30A binds to P4-ATPase, which participates in the migration process of tumor cells. The enriched functions (Table 3) and pathways (Table 4) of our predicted signaling network, including regulation of the actin cytoskeleton, adherens junctions, and focal adhesion, are already known to be related to migration, which increases the credibility of our predicted network.

As indicated by our results, the mRNA expression levels of *SRC*, *CDC42*, *WASL*, and *RHO* were all changed during cancer cell migration (Fig 4A and 4B). *SRC* is a proto-oncogene that is aberrantly activated in most types of cancer [29], which is consistent with our results showing that *SRC* is significantly increased in both cell types. Further, the FAK-SRC signaling pathway regulates the invasion of lung cancer [30] and Ewing sarcoma cells [29], indicating that SRC may be a key therapeutic target for cancer treatment. It is widely accepted that all modes of migration require RHO GTPase, including RHO and CDC42 (Fig 4A and 4B) due to its effects on the regulation of actin dynamics that plays a critical role in cell migration depending on the environment [31, 32]. It has been reported that enhanced activity of RHO stimulates the *in*
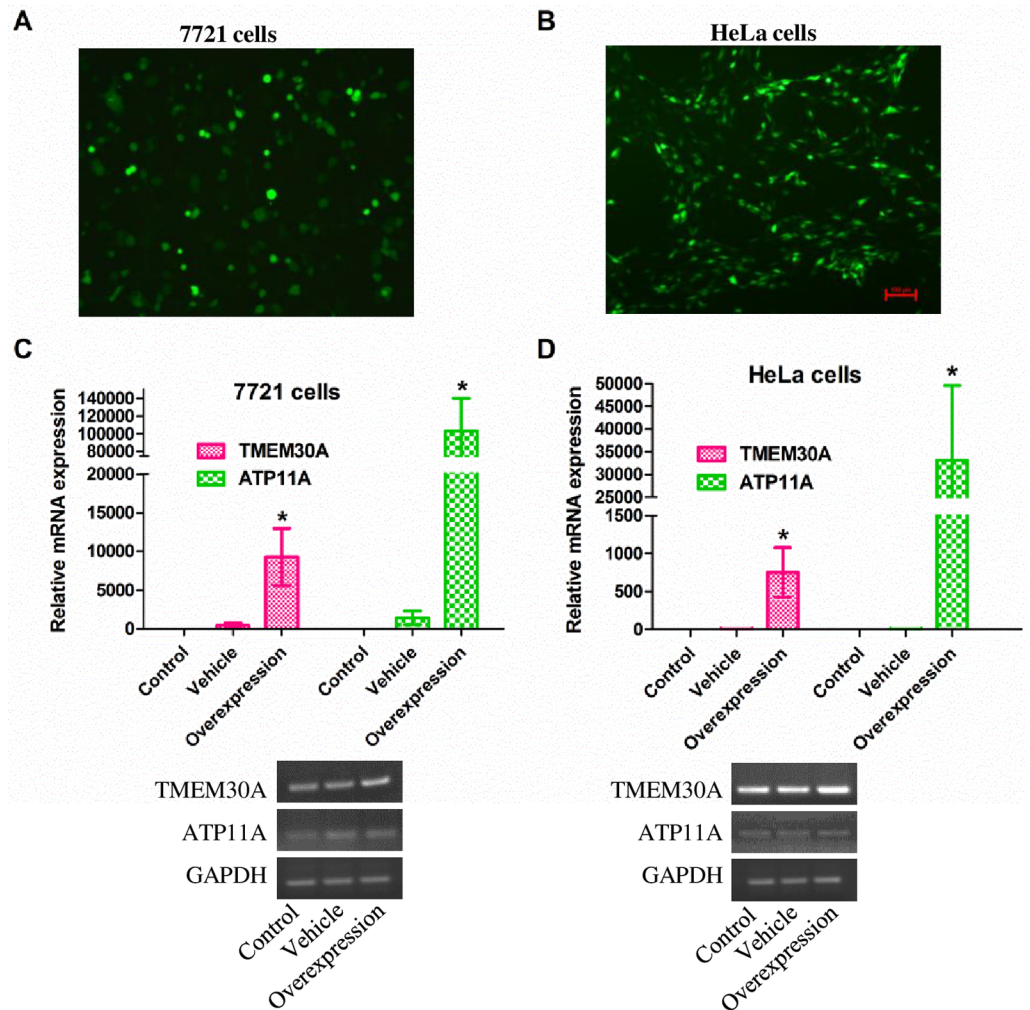
Fig 2. Identification of the overexpression of TMEM30A and ATP11A in 7721 or HeLa cells. (A and B) 7721 or HeLa cells were viewed under a Nikon fluorescence microscope 24 hours following transfection with vectors capable of expressing green fluorescent protein (GFP) fusion proteins. (C and D) The mRNA levels of TMEM30A and ATP11A were assessed by qPCR in 7721 or HeLa cells. The products of the qPCR were separated on 1.5% agarose gels and visualized using ethidium bromide staining. Abundance of each mRNA transcript is expressed relative to GAPDH as an internal control. Data are represented as the mean ± SEM. n = 4. *, $p < 0.05$; Overexpression vs. Vehicle.

vitro migration of papillary thyroid cancer (PTC) [33], hepatocellular carcinoma [34] and human colon cancer cells [35]. CDC42 plays an important role in the establishment of cell migratory polarity and persistence via its activation in clear cell renal cell carcinoma (ccRCC) [36]. This is consistent with our results showing that upregulation of CDC42 and RHO promotes the migration of 7721 and HeLa cells. In addition, there was an expression change in WASL, an effector of the Rho protein, which was dramatically decreased in HeLa cells and increased in 7721 cells. WASL is a regulator of actin polymerization and is responsible for membrane ruffling [37]. The reverse expression of *WASL* in these two tumor cell lines implies a complicated function of *WASL* in different cancer types. According to the literature, knockdown of *WASL* significantly reduces the number of membrane protrusions and inhibits breast cancer cell invasiveness [38], whereas increased WASL promotes lymph node metastasis [38].
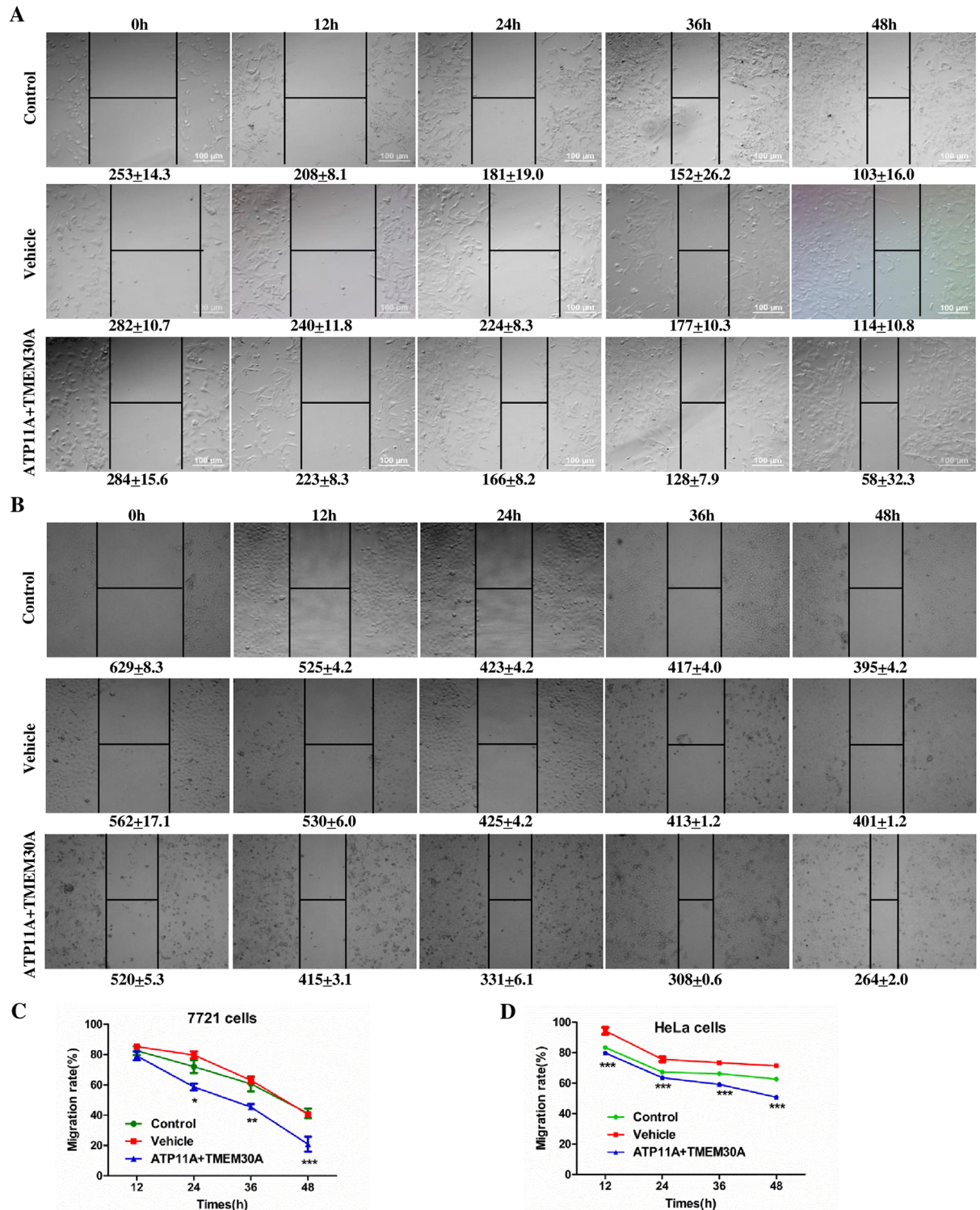
Fig 3. Effect of TMEM30A and ATP11A on 7721 or HeLa cell migration using an wound-healing assay. Representative images of the scratched areas in each condition at different time points were photographed. (A and B) Average gaps in three groups of 7721 or HeLa cells, respectively. (C and D) Statistical analysis of the migration rate in three groups of 7721 or HeLa cells, respectively. Data are represented as the mean ± SEM. 7721 cells, n = 6; HeLa cells, n = 3. *, $p < 0.05$; **, $p < 0.01$; ***, $p < 0.001$; ATP11A+TMEM30A vs. Vehicle.

https://doi.org/10.1371/journal.pone.0179900.g003
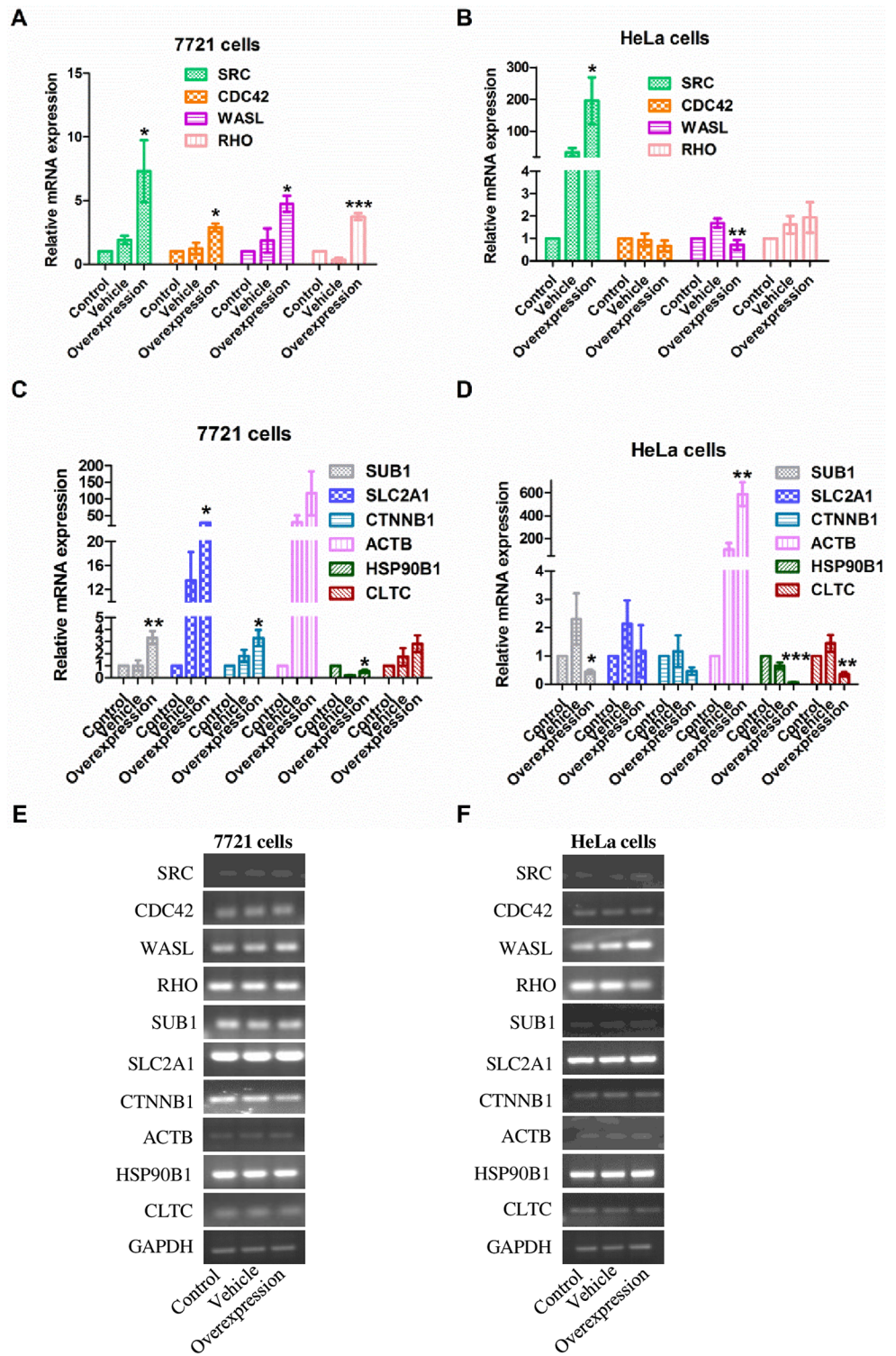
Fig 4. The expression of ten genes was evaluated by qPCR in 7721 or HeLa cells. The overexpression group represents the coexpressed TMEM30A and ATP11A. (A and B) The 4 genes collected from the literature were assessed by qPCR in the control group, vehicle group, and overexpression group, in 7721 or HeLa cells. (C and D) The 6 predicted genes were assessed by qPCR in the control group, vehicle group, and overexpression group, in 7721 or HeLa cells. (E and F) The products of the qPCR were separated on 1.5% agarose gels and visualized by ethidium bromide staining. Abundance of each mRNA transcript is expressed relative to GAPDH as an internal control. Data are represented as the mean ± SEM. n = 4. *, $p < 0.05$; **, $p < 0.01$; ***, $p < 0.001$; Overexpression vs. Vehicle.

The same reverse expression was also found with *SUB1*, which suggests that further experiments are needed to clarify the involvement of these two genes in tumor migration.

Furthermore, the expression of *SLC2A1*, *CTNNB1*, *ACTB*, and *CLTC* were significantly changed in only one type of cancer during migration (Fig 4C and 4D). For instance, ACTB is a highly conserved protein well-known for its regulation of the actin cytoskeleton and adherens junctions, which are necessary for both normal and tumor cell migration [31, 39]. The significant change in the expression level of ACTB in HeLa cells indicates that ACTB may execute a special function in HeLa cell migration. In addition, SLC2A1 is a transporter that facilitates glucose entering the cytoplasm [40]. It is critical for the growth, proliferation, and migration of tumor cells, and its high expression is associated with hepatocellular carcinoma [40] and poor cancer survival [22]. Hepatocellular carcinoma cells were used in our experiments, with a consistent change in mRNA levels being observed by qPCR (Fig 4C). Moreover, CLTC, a membrane protein like TMEM30A and its partner P4-ATPase [24], is expressed in pancreatic cancer cells and tumor blood vessels [41], being involved in the ubiquitous uptake of a variety of macromolecules, membrane transporters, and adhesion molecules [41, 42]. According to our results, CLTC was dramatically decreased in HeLa cells following overexpression of TMEM30A, indicating involvement in HeLa cell migration, and implying that TMEM30A and its partner P4-ATPase, may function together with CLTC on the membrane to trigger downstream signaling pathways involved in tumor migration. The slight difference in the expression of these genes in different cancer cell types also suggests the delicate and complex regulatory mechanisms involved in tumor cell migration, implying that anti-cancer therapeutics are complicated and highly dependent on cell type. Interestingly, considering that the overexpression of TMEM30A promotes the migration of these two types of cancer cells, TMEM30A may be a novel therapeutic target in cancer treatment.

Proteins from the same signaling pathway are usually co-expressed, in addition, the results of our biological verification experiments showed that the mRNA levels of the selected genes changed along with increased expression of TMEM30A, therefore, novel signaling pathway could be predicted by differentially expressed genes from proteomic data [28]. Although the protein-protein interactions are undirected, signaling transduction is normally the process by which a signal is transmitted through the cell as a series of molecular events. Proteins responsible for detecting stimuli are generally located on the plasma membrane, and changes in protein phosphorylation state give rise to a cascade of biochemical events mediated by protein kinase, which ultimately regulate the function of transcription factors. Furthermore, many researchers have also developed various algorithms and tools to infer signaling pathways using the protein-protein interactions deposited in public database [26, 43, 44]. Thus, we could infer the direction that we verified experimentally to be in the following order: transmembrane protein (ATP11B, TMEM30A, CLTC, RHO), cytoplasmic protein (WASL, CDC42, ACTB, SEC23A, HSP90B1, CTNNB1), kinase (SRC), transcription factor activator (SUB1) (S2 Fig).

In conclusion, by combining the predictive power of computational biology and molecular biology experiments, we successfully identified the migration-related signaling network involved in the TMEM30A complex, and the randomly selected genes were subsequently validated and shown to indeed be regulated by TMEM30A during tumor migration. In particular, we found that TMEM30A regulates several migration-related genes including *SUB1*, *SLC2A1*, *CTNNB1*, *ACTB*, and *CLTC* during tumor migration, which further demonstrates the effectiveness of our proposed method. We believe that our identified signaling network can shed light on the regulatory mechanisms underlying tumor migration and facilitate the understanding of the molecular basis of tumor invasion.

Supporting information

S1 Fig. A flowchart of the molecular signaling networks identified to be involved in the TMEM30A complex during tumor migration by exploring the PPIN and known genes in the literature.
(TIF)

S2 Fig. The verified signaling pathway extracted from the whole PIN.
(TIF)

S1 Table. Primary data used in Fig 2.
(XLSX)

S2 Table. Primary data used in Fig 3.
(XLSX)

S3 Table. Primary data used in Fig 4.
(XLSX)

S1 File. Original and unadjusted gels for products identification after qPCR.
(PPTX)

Acknowledgments

Author Contributions

Conceptualization: JW TQW JX.

Formal analysis: QW DFL FFZ DW.

Investigation: JW QW FFZ DW.

Resources: RLF RM.

Writing – original draft: JW QW.

Writing – review & editing: KW.

References

1. Zimmermann M, Box C, Eccles SA. Two-dimensional vs. three-dimensional in vitro tumor migration and invasion assays. Methods in molecular biology. 2013; 986:227–52. https://doi.org/10.1007/978-1-62703-311-4_15 PMID: 23436416.

2. Kikkawa Y, Harashima N, Ikari K, Fujii S, Katagiri F, Hozumi K, et al. Down-regulation of cell adhesion via rho-associated protein kinase (ROCK) pathway promotes tumor cell migration on laminin-511. Experimental cell research. 2016; 344(1):76–85. https://doi.org/10.1016/j.yexcr.2016.04.002 PMID: 27068375.

3. Zhang D, Zhao L, Shen Q, Lv Q, Jin M, Ma H, et al. Down-regulation of KIAA1199/CEMIP by miR-216a suppresses tumor invasion and metastasis in colorectal cancer. International journal of cancer. 2017; 140(10):2298–309. https://doi.org/10.1002/ijc.30656 PMID: 28213952.

4. Krakhmal NV, Zavyalova MV, Denisov EV, Vtorushin SV, Perelmuter VM. Cancer Invasion: Patterns and Mechanisms. Acta naturae. 2015; 7(2):17–28. PMID: 26085941;

5. Abdoli G, Bottai M, Sandelin K, Moradi T. Breast cancer diagnosis and mortality by tumor stage and migration background in a nationwide cohort study in Sweden. Breast. 2017; 31:57–65. https://doi.org/10.1016/j.breast.2016.10.004 PMID: 27810701.

6. Diermeier SD, Chang KC, Freier SM, Song J, El Demerdash O, Krasnitz A, et al. Mammary Tumor-Associated RNAs Impact Tumor Cell Proliferation, Invasion, and Migration. Cell reports. 2016; 17(1):261–74. https://doi.org/10.1016/j.celrep.2016.08.081 PMID: 27681436;

7. Jacquemet G, Hamidi H, Ivaska J. Filopodia in cell adhesion, 3D migration and cancer cell invasion. Current opinion in cell biology. 2015; 36:23–31. https://doi.org/10.1016/j.ceb.2015.06.007 PMID: 26186729.

8. Clark AG, Vignjevic DM. Modes of cancer cell invasion and the role of the microenvironment. Current opinion in cell biology. 2015; 36:13–22. https://doi.org/10.1016/j.ceb.2015.06.004 PMID: 26183445.

9. Devis L, Moiola CP, Masia N, Martinez-Garcia E, Santacana M, Stirbat TV, et al. Activated leukocyte cell adhesion molecule (ALCAM) is a marker of recurrence and promotes cell migration, invasion, and metastasis in early-stage endometrioid endometrial cancer. The Journal of pathology. 2017; 241 (4):475–87. https://doi.org/10.1002/path.4851 PMID: 27873306.

10. He X, Wang L, Riedel H, Wang K, Yang Y, Dinu CZ, et al. Mesothelin promotes epithelial-to-mesenchymal transition and tumorigenicity of human lung cancer and mesothelioma cells. Molecular cancer. 2017; 16(1):63. https://doi.org/10.1186/s12943-017-0633-8 PMID: 28288645;

11. Khajah MA, Al Saleh S, Mathew PM, Luqmani YA. Differential effect of growth factors on invasion and proliferation of endocrine resistant breast cancer cells. PloS one. 2012; 7(7):e41847. https://doi.org/10.1371/journal.pone.0041847 PMID: 22860018;

12. Fujino Y, Takeishi S, Nishida K, Okamoto K, Muguruma N, Kimura T, et al. Downregulation of micro-RNA-100/microRNA-125b is associated with lymph node metastasis in early colorectal cancer with submucosal invasion. Cancer Sci. 2017; 108(3):390–7. https://doi.org/10.1111/cas.13152 PMID: 28032929;

13. Li Z, Hou P, Fan D, Dong M, Ma M, Li H, et al. The degradation of EZH2 mediated by lncRNA ANCR attenuated the invasion and metastasis of breast cancer. Cell death and differentiation. 2017; 24(1):59–71. https://doi.org/10.1038/cdd.2016.95 PMID: 27716745;

14. Liang WC, Fu WM, Wong CW, Wang Y, Wang WM, Hu GX, et al. The lncRNA H19 promotes epithelial to mesenchymal transition by functioning as miRNA sponges in colorectal cancer. Oncotarget. 2015; 6 (26):22513–25. https://doi.org/10.18632/oncotarget.4154 PMID: 26068968;

15. Kpetemey M, Chaudhary P, Van Treuren T, Vishwanatha JK. MIEN1 drives breast tumor cell migration by regulating cytoskeletal-focal adhesion dynamics. Oncotarget. 2016; 7(34):54913–24. https://doi.org/10.18632/oncotarget.10798 PMID: 27462783;

16. Zhang X, Yuan X, Shi H, Wu L, Qian H, Xu W. Exosomes in cancer: small particle, big player. Journal of hematology & oncology. 2015; 8:83. https://doi.org/10.1186/s13045-015-0181-x PMID: 26156517;

17. Te Boekhorst V, Friedl P. Plasticity of Cancer Cell Invasion-Mechanisms and Implications for Therapy. Advances in cancer research. 2016; 132:209–64. https://doi.org/10.1016/bs.acr.2016.07.005 PMID: 27613134.

18. Wang J, Li X, Cheng H, Wang K, Lu W, Wen T. Overexpression of Rho-GDP-dissociation inhibitor-gamma inhibits migration of neural stem cells. Journal of neuroscience research. 2013; 91(11):1394–401. https://doi.org/10.1002/jnr.23261 PMID: 23996536.

19. Folmer DE, Mok KS, de Wee SW, Duijst S, Hiralall JK, Seppen J, et al. Cellular localization and biochemical analysis of mammalian CDC50A, a glycosylated beta-subunit for P4 ATPases. The journal of histochemistry and cytochemistry: official journal of the Histochemistry Society. 2012; 60(3):205–18. https://doi.org/10.1369/0022155411435705 PMID: 22253360;

20. Kato U, Inadome H, Yamamoto M, Emoto K, Kobayashi T, Umeda M. Role for phospholipid flippase complex of ATP8A1 and CDC50A proteins in cell migration. The Journal of biological chemistry. 2013; 288(7):4922–34. https://doi.org/10.1074/jbc.M112.402701 PMID: 23269685;

21. Wang J, Hu F, Cheng H, Zhao XM, Wen T. A systems biology approach to identify the signalling network regulated by Rho-GDI-gamma during neural stem cell differentiation. Molecular bioSystems. 2012; 8(11):2916–23. https://doi.org/10.1039/c2mb25147g PMID: 22892720.

22. Fan J, Zhou JQ, Yu GR, Lu DD. Glucose transporter protein 1-targeted RNA interference inhibits growth and invasion of the osteosarcoma cell line MG63 in vitro. Cancer biotherapy & radiopharmaceuticals. 2010; 25(5):521–7. https://doi.org/10.1089/cbr.2010.0784 PMID: 20854211.

23. Li C, Zhao L, Chen Y, He T, Chen X, Mao J, et al. MicroRNA-21 promotes proliferation, migration, and invasion of colorectal cancer, and tumor growth associated with down-regulation of sec23a expression. BMC cancer. 2016; 16:605. https://doi.org/10.1186/s12885-016-2628-z PMID: 27495250;

24. Vestergaard AL, Mikkelsen SA, Coleman JA, Molday RS, Vilsen B, Andersen JP. Specific mutations in mammalian P4-ATPase ATP8A2 catalytic subunit entail differential glycosylation of the accessory CDC50A subunit. FEBS letters. 2015; 589(24 Pt B):3908–14. https://doi.org/10.1016/j.febslet.2015.11.031 PMID: 26592152.

25. Miyoshi N, Ishii H, Mimori K, Tanaka F, Nagai K, Uemura M, et al. ATP11A is a novel predictive marker for metachronous metastasis of colorectal cancer. Oncology reports. 2010; 23(2):505–10. PMID: 20043114.

26. Segal E, Wang H, Koller D. Discovering molecular pathways from protein interaction and gene expression data. Bioinformatics. 2003; 19 Suppl 1:i264–71. PMID: 12855469.

27. Ji Z, Wu D, Zhao W, Peng H, Zhao S, Huang D, et al. Systemic modeling myeloma-osteoclast interactions under normoxic/hypoxic condition using a novel computational approach. Scientific reports. 2015; 5:13291. https://doi.org/10.1038/srep13291 PMID: 26282073;

28. Ji Z, Su J, Liu C, Wang H, Huang D, Zhou X. Integrating genomics and proteomics data to predict drug effects using binary linear programming. PloS one. 2014; 9(7):e102798. https://doi.org/10.1371/journal.pone.0102798 PMID: 25036040;

29. Indovina P, Casini N, Forte IM, Garofano T, Cesari D, Iannuzzi CA, et al. SRC Family Kinase Inhibition in Ewing Sarcoma Cells Induces p38 MAP Kinase-Mediated Cytotoxicity and Reduces Cell Migration. Journal of cellular physiology. 2017; 232(1):129–35. https://doi.org/10.1002/jcp.25397 PMID: 27037775.

30. Chikara S, Lindsey K, Borowicz P, Christofidou-Solomidou M, Reindl KM. Enterolactone alters FAK-Src signaling and suppresses migration and invasion of lung cancer cell lines. BMC complementary and alternative medicine. 2017; 17(1):30. https://doi.org/10.1186/s12906-016-1512-3 PMID: 28068967;

31. Ridley AJ. Rho GTPase signalling in cell migration. Current opinion in cell biology. 2015; 36:103–12. https://doi.org/10.1016/j.ceb.2015.08.005 PMID: 26363959;

32. Zegers MM, Friedl P. Rho GTPases in collective cell migration. Small GTPases. 2014; 5:e28997. https://doi.org/10.4161/sgtp.28997 PMID: 25054920;

33. Li JJ, Sun ZJ, Yuan YM, Yin FF, Bian YG, Long LY, et al. EphB3 Stimulates Cell Migration and Metastasis in a Kinase-dependent Manner through Vav2-Rho GTPase Axis in Papillary Thyroid Cancer. The Journal of biological chemistry. 2017; 292(3):1112–21. https://doi.org/10.1074/jbc.M116.750349 PMID: 27986811;

34. Ahronian LG, Zhu LJ, Chen YW, Chu HC, Klimstra DS, Lewis BC. A novel KLF6-Rho GTPase axis regulates hepatocellular carcinoma cell migration and dissemination. Oncogene. 2016; 35(35):4653–62. https://doi.org/10.1038/onc.2016.2 PMID: 26876204;

35. Becker MS, Muller PM, Bajorat J, Schroeder A, Giaisi M, Amin E, et al. The anticancer phytochemical rocaglamide inhibits Rho GTPase activity and cancer cell migration. Oncotarget. 2016; 7(32):51908–21. https://doi.org/10.18632/oncotarget.10188 PMID: 27340868;

36. Wang K, Sun Y, Tao W, Fei X, Chang C. Androgen receptor (AR) promotes clear cell renal cell carcinoma (ccRCC) migration and invasion via altering the circHIAT1/miR-195-5p/29a-3p/29c-3p/CDC42 signals. Cancer letters. 2017; 394:1–12. https://doi.org/10.1016/j.canlet.2016.12.036 PMID: 28089832.

37. Wang WS, Zhong HJ, Xiao DW, Huang X, Liao LD, Xie ZF, et al. The expression of CFL1 and N-WASP in esophageal squamous cell carcinoma and its correlation with clinicopathological features. Diseases of the esophagus: official journal of the International Society for Diseases of the Esophagus. 2010; 23 (6):512–21. https://doi.org/10.1111/j.1442-2050.2009.01035.x PMID: 20095995.

38. Schwickert A, Weghake E, Bruggemann K, Engbers A, Brinkmann BF, Kemper B, et al. microRNA miR-142-3p Inhibits Breast Cancer Cell Invasiveness by Synchronous Targeting of WASL, Integrin Alpha V, and Additional Cytoskeletal Elements. PloS one. 2015; 10(12):e0143993. https://doi.org/10.1371/journal.pone.0143993 PMID: 26657485;

39. Poulter NS, Thomas SG. Cytoskeletal regulation of platelet formation: Coordination of F-actin and microtubules. The international journal of biochemistry & cell biology. 2015; 66:69–74. https://doi.org/10.1016/j.biocel.2015.07.008 PMID: 26210823.

40. Sun HW, Yu XJ, Wu WC, Chen J, Shi M, Zheng L, et al. GLUT1 and ASCT2 as Predictors for Prognosis of Hepatocellular Carcinoma. PloS one. 2016; 11(12):e0168907. https://doi.org/10.1371/journal.pone.0168907 PMID: 28036362;

41. Tung KH, Lin CW, Kuo CC, Li LT, Kuo YH, Lin CW, et al. CHC promotes tumor growth and angiogenesis through regulation of HIF-1alpha and VEGF signaling. Cancer letters. 2013; 331(1):58–67. https://doi.org/10.1016/j.canlet.2012.12.001 PMID: 23228632.

42. Schmid SL. Clathrin-mediated endocytosis: a universe of new questions. Molecular biology of the cell. 2010; 21(22):3818–9. https://doi.org/10.1091/mbc.E10-05-0386 PMID: 21079028;

43. Wang K, Hu F, Xu K, Cheng H, Jiang M, Feng R, et al. CASCADE_SCAN: mining signal transduction network from high-throughput data based on steepest descent method. BMC Bioinformatics. 2011; 12:164. https://doi.org/10.1186/1471-2105-12-164 PMID: 21575263;

44. Zhao XM, Wang RS, Chen L, Aihara K. Automatic modeling of signaling pathways by network flow model. J Bioinform Comput Biol. 2009; 7(2):309–22. PMID: 19340917.